Available online at www.sciencedirect.com
SCIENCE DIRECT®
Journal of Nuclear Materials 355 (2006) 68–82
journal of nuclear materials
www.elsevier.com/locate/jnucmat

Sensitization behaviour of modified 316N and 316L stainless steel weld metals after complex annealing and stress relieving cycles

N. Parvathavarthini [a], R.K. Dayal [a,*], H.S. Khatak [a], V. Shankar [b], V. Shanmugam [b]

[a] *Indira Gandhi Centre for Atomic Research, Corrosion Science and Technology Division, Materials Characterisation Group, Kalpakkam, Tamil Nadu 603 102, India*

[b] *Materials Technology Division, Materials Development Group, Indira Gandhi Centre for Atomic Research, Kalpakkam – 603 102 Tamil Nadu, India*

Received 15 September 2005; accepted 20 April 2006

Abstract

Sensitization behaviour of austenitic stainless steel weld metals prepared using indigenously developed modified 316N (C = 0.05%; N = 0.12%) and 316L (C = 0.02%; N = 0.07%) electrodes was studied. Detailed optical and scanning electron microscopic examination was carried out to understand the microstructural changes occurring in the weld metal during isothermal exposure at various temperatures ranging from 500 °C to 850 °C (773–1123 K). Based on these studies the mechanism of sensitization in the austenite–ferrite weld metal has been explained. Time–temperature–sensitization (TTS) diagrams were established using ASTM A262 Practice *E* test. From the TTS diagrams, critical cooling rate (CCR) above which there is no risk of sensitization was calculated for both materials. The heating/cooling rates to be followed for avoiding sensitization during heat treatment cycles consisting of solution-annealing and stress-relieving in fabrication of welded components of AISI 316LN stainless steel (SS) were estimated taking into account the soaking time and the number of times the component undergoes thermal excursions in the sensitization regime. The results were validated by performing controlled heating and cooling heat treatment trials on welded specimens.

1. Introduction

AISI 316LN SS (C = 0.024–0.03% and N = 0.06–0.08%) has been chosen as the primary structural material for the 500 MWe Prototype Fast Breeder Reactor (PFBR) being built at Kalpakkam. Welding is extensively employed in the fabrication of PFBR components. Sensitization in the base metal is not a problem at the heat-affected zone of 316LN SS weldments because carbon content of the base material is ⩽0.03%. Normally, the weld metal does not get sensitized because of the duplex austenite–ferrite structure in which chromium depletion due to carbide precipitation does not

* Corresponding author. Tel.: +91 44 27480121; fax: +91 44 27480081.
E-mail address: rkd@igcar.gov.in (R.K. Dayal).

0022-3115/$ - see front matter © 2006 Elsevier B.V. All rights reserved.
doi:10.1016/j.jnucmat.2006.04.006

readily occur. Even if carbide precipitation takes place, rapid diffusion of chromium from the chromium-rich delta ferrite phase results in quicker homogenisation. However, this immunity from sensitization and subsequent intergranular corrosion (IGC) can be severely compromised especially on heat treatment in the temperature range of transformation. The severity of this problem depends on the carbon content as well as the extent to which the duplex structure is lost through the dissolution of ferrite. For PFBR components welding of the AISI 316LN SS is to be carried out using modified 316N (as per AISI/AWS SFA-5.4) electrodes developed indigenously. Weld metal cracking is controlled by optimizing the chemical composition of the welding consumables. Carbon in the range of 0.045–0.055% and nitrogen in the range of 0.06–0.1% are specified to provide weld joints with improved creep strength and freedom from sensitization in the as-welded state. In addition the ferrite content in the weld metal is specified to be between 3 and 7 FN (measured magnetically) to promote ferrite solidification mode.

Following three types of heat treatments are required for austenitic stainless steel components [1]:

(i) *Solution-annealing* at 1050 °C (1323 K) or above for full stress-relieving, restoration of mechanical properties and corrosion resistance particularly when the maximum allowable level of cold work is exceeded. Following this treatment, slow cooling is necessary to avoid reintroduction of residual stress. When the welded components are solution-annealed, delta ferrite dissolves and the weld metal behaviour is similar to that of austenitic base metal of higher carbon content (~0.05% as against 0.03% max. in base metal) for which CCR to avoid sensitization is much higher than that of the base metal. Therefore, it becomes necessary to optimize the heating and cooling cycles to avoid sensitization as well as to preclude reintroduction of residual stresses.

(ii) Some components of PFBR encounter wear (adhesive or abrasive) due to sliding movement and erosion due to high velocity sodium. Nickel base, cobalt-free hard facing is used for mating parts in most of the nuclear steam system components. *Stress-relieving* at 750–850 °C (1023–1123 K) is required after hard facing because of the high stresses built-up at the coating-substrate interface. Without this heat treatment cracking of the coating can take place during inservice thermal cycling because of the mismatch between the expansion coefficients of the hard face coating and stainless steel substrate.

(iii) *Dimensional stabilization* treatment is required for relieving peak residual stresses and is performed before final machining to prevent distortion during final machining and assembly. It is performed at a temperature 50 °C above the expected peak transient temperature (the highest temperature the component is likely to experience for short duration of time during service).

According to ASM hand book [2], heat treatment periods of 3–4 h per 25 mm are used for dimensional stabilization treatment and 1 h per 25 mm is used for solution-annealing treatment. Heating and cooling rates are to be controlled because very fast cooling rates will result in distortion and reintroduction of residual stress, while too slow a cooling will lead to sensitization. Hence optimum heating/cooling rates are to be established for welded components.

A large volume of literature exists with reference to carbide precipitation and sensitization behaviour of austenitic stainless steel base metals [3–7], where nucleation of the carbide phase requires a certain incubation period. Sensitization kinetics in the molybdenum-containing grades such as 316N and 316L are governed by the carbon and nitrogen contents [5]. Duplex stainless steels represent a different situation where the large area of austenite/ferrite interphase interfaces serves to reduce the barrier to nucleation and the precipitation kinetics are faster [8]. In duplex stainless steels, precipitation of chromium carbides and nitrides leads to pitting corrosion [9], while sigma phase formation increases susceptibility to stress corrosion cracking [10]. Austenitic weld metal with only a few percent of retained ferrite phase represents an intermediate situation with reference to both these cases. While the predominantly austenitic structure renders the material susceptible to sensitization by chromium depletion, some amount of protection from these phenomena is afforded by the ferrite present in welds [11] and castings [12]. The amount of ferrite present and therefore the austenite/ferrite interfacial area can decrease significantly with heat

treatment through transformation of the ferrite to austenite, carbide and sigma phase. Under such conditions, austenitic stainless steel weld metal and welded components normally immune to sensitization, can be rendered susceptible to corrosion attack [13]. Sensitization data on austenitic stainless steel weld metal is scarce. In the present case, the complex manufacturing cycle necessitated establishment of time–temperature–sensitization (TTS) diagrams, calculation of CCR from TTS diagrams and validation of the estimated CCR. Validation was performed taking into account the number of times the component undergoes thermal excursions in sensitization regime with various soaking times by performing controlled heating/cooling heat treatments as necessary. To begin with, systematic investigations were carried out to understand the sensitization behaviour by establishing the TTS diagram for the weld metal prepared using modified 316N and 316L electrodes. Detailed microstructural characterisation of the various heat treated specimens has been carried out using optical and scanning electron microscopy to explain the mechanism of sensitization in modified 316N and 316L stainless steel weld metals.

2. Experimental

Weld pads were prepared by Shielded Metal Arc Welding (SMAW) process using modified 316N electrodes (3.15 mm diameter) and 316L (3.15 mm diameter) of M/s. Mailam India Ltd., and the welding parameters used are presented in Tables 1a and 1b. The chemical composition of the weld metals was analysed using optical emission spectroscopy and the results are given in Tables 2a and 2b. The equipment used was Jobin Yvon make model JY-132 F. Liquid penetrant and radiographic examinations were performed to ensure that the weld pads were free from porosity and defects. From the weld pads, specimens of dimensions $80 \times 10 \times 3$ mm were cut for sensitization studies as per ASTM Standard A262 Practice *E* test. Delta ferrite measurements were carried out using Ferritescope. Specimens

Table 1a
Welding parameters for modified 316N SS weld metal

No. of passes	Arc voltage (V)	Arc current (A)	Speed (mm/min)	Heat input (J/mm)
1	22–23	115–120	160	991
2	22–23	115–120	186	852
3–16	21–22	120–130	160	1008
17–26	21–22	130–140	290	600

Table 1b
Welding parameters for modified 316L SS weld metal

Pad no.	Arc voltage (V)	Arc current (A)	Speed (mm/min)	Heat input (J/mm)
1	20	80	180–200	480–533
2	20–24	90–100	180–210	540–735
3	20	80–90	170–210	457–568
4	24–26	100–110	170–220	720–918

Table 2a
Chemical composition for modified 316N SS weld metal

Element	Wt.%
Carbon	0.050
Nitrogen	0.120
Chromium	18.5
Nickel	11.1
Molybdenum	1.9
Manganese	1.4
Silicon	0.46
Sulphur	0.006
Phosphorus	0.025
Tantalum	<0.010
Titanium	23 ppm
Niobium	<0.07
Vanadium	0.075
Boron	<10 ppm
Copper	0.210
Cobalt	0.060
Delta ferrite	
As per WRC 92	1.8 FN
By Ferritescope	3.5, [4.1, 3.9] FN

Table 2b
Chemical composition for modified 316L SS weld metal

Element	Wt.%
Carbon	0.020
Nitrogen	0.070
Chromium	18.5
Nickel	11.5
Molybdenum	2.3
Manganese	1.6
Silicon	0.28
Sulphur	0.009
Phosphorus	0.045
Titanium	<0.080
Niobium	<0.070
Vanadium	0.075
Copper	0.210
Cobalt	0.060
Delta ferrite	8–11 FN

Table 3
Delta ferrite content of modified 316L SS weld metal after various heat treatments

Temp./time	Ferrite number				
	24 h	40 h	50 h	100 h	200 h
625 °C (898 K)	–	–	5.27	2.67	1.74
650 °C (923 K)	3.86	2.94	2.68	1.18	–
675 °C (948 K)	–	–	1.10	0.36	0.04

made from weld pads prepared using 316N electrodes were heat treated at various temperatures ranging from 500 °C to 850 °C (773–1123 K) for various durations ranging from 20 min to 20 h. Specimens made from weld pads prepared using 316L electrodes were heat treated at 625 °C (898 K), 650 °C (923 K) and 675 °C (948 K) for durations ranging from 24 h to 200 h. Changes in delta ferrite content after ageing treatment of 316L SS weld metal are presented in Table 3.

The heat treated specimens were electrolytically etched in 10% oxalic acid for a few seconds at 2 V in order to reveal the microstructure. Optical and scanning electron microscopic examination was carried out for characterising the microstructure. The specimens were analysed for the possible formation of secondary phases. Bulk extraction of the precipitates was carried out for modified 316N SS weld specimens by keeping the specimens at 1.5 V with respect to platinum cathode in 10% Hydrochloric acid – 90% methanol solution for a duration of 24 h. This results in selective dissolution of austenite phase [14], while carbides and other secondary phases remain undissolved and were collected by centrifuging. The extracted powder samples were washed in methanol, dried and analysed by X-ray diffraction technique using Cu K_α radiation. The modified 316L SS weld specimens were etched in modified Murakami reagent for 15 s to reveal secondary intermetallic phases such as sigma and chi.

All the heat treated specimens were tested to determine occurrence of sensitization as per ASTM standard A262 practice *E* [15]. According to this standard, the specimen to be tested was embedded in copper turnings and exposed to boiling copper sulphate–sulphuric acid solution for 24 h. Then the specimens were bent slowly through 90° angle around a mandrel of 6 mm diameter. Those specimens in which cracks were observed in the bent portion at a magnification of 20× were categorised as sensitized.

3. Results and discussion

3.1. Development of TTS diagram

The results obtained for the various heat treated specimens in the ASTM standard A262 practice *E* for modified 316N SS weld metal and modified 316L SS weld metal are collectively presented in a TTS diagram in Fig. 1. Sensitized specimens with cracks after exposure and bending are indicated by closed circles. Specimens with no cracking in the bent portion were adjudged free from sensitization (points marked X). From these data points, sensitized and non-sensitized area are separated by drawing a smooth curve such that the curve represents the beginning of sensitization process. Efforts were made to keep all the non-sensitized data points outside the curve except one data point at 550 °C (823 K) which has fallen on the curve. This has happened in order to maintain the smoothness of the curve. By drawing the curve in this way it is ensured that there is no data point outside the curve which will show sensitization.

From the diagram, it is clear that the modified 316N SS weld metal gets sensitized in the temperature range of 625–725 °C (898–998 K). The minimum time required for sensitization at the nose temperature (t_{min}) is about 25 min. From the data, the CCR above which there is no risk of sensitization, was calculated using the method developed by Dayal and Gnanamoorthy [16]. From these calculations, the CCR for weld metal was determined as 160 °C/h. This critical cooling rate is applicable only when cooling of the weld metal starts from 725 °C (998 K).

It can be seen that the 316L SS weld metal gets sensitized in the temperature range of 625–675 °C

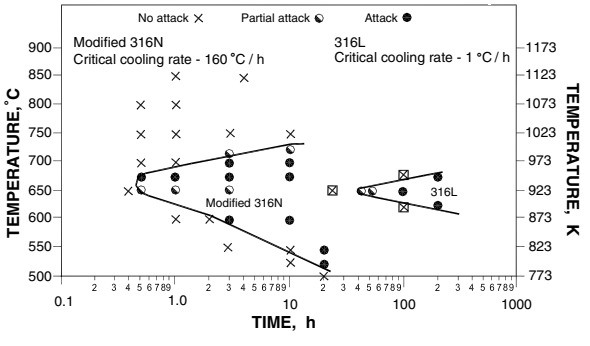

Fig. 1. Time–temperature–sensitization diagrams for modified 316N SS weld metal and 316L SS weld metal.

(898–948 K). The minimum time required for sensitization at the nose temperature (t_{min}) is about 40 h. From this diagram, CCR above which there is no risk of sensitization, was calculated as 1 °C/h. This value is applicable only when cooling of the weld metal starts from 675 °C (948 K).

3.2. Microstructural changes during heat treatment

3.2.1. Modified 316N stainless steel weld metal

The initial microstructure of modified 316N SS weld metal specimen is presented in Fig. 2. Duplex austeno-ferritic structure with delta ferrite of vermicular morphology can be clearly seen in the microstructure. Delta ferrite was estimated to be in the range of 3.5–4.1 FN when measured using Ferritescope on the top bead. However, in some regions of the multipass weld metal, considerable transformation of the ferrite had taken place. In these regions, nucleation of $M_{23}C_6$ carbide is expected in the as-welded condition itself by exposure to the temperature range of 450–750 °C (723–1023 K) by thermal cycling during multipass welding. The heat treatments given subsequently to the test specimens served to further transform the ferrite to various extents depending upon the temperature and time of exposure.

When heat treated at 525 °C (798 K) for 10–15 h, the delta ferrite has transformed to carbides and austenite and growth of $M_{23}C_6$ carbides along delta ferrite/austenite (δ/γ) boundaries has taken place. This is presented in Figs. 3(a) and 3(b), respectively, for 10 h and 15 h exposure. Initially, the carbide film is continuous (Fig. 3(a)), which is shown by the darkening of the δ/γ boundary. The delta ferrite grains are also considerably intact, while in Fig. 3(b), most of the delta ferrite phase has transformed and the remaining phases in the intercellular regions are carbide particles, as shown by discrete particles with dark appearance on etching with 10% oxalic acid. Precipitation of intermetallic phases such as sigma or chi phase is not expected at this temperature [17,18]. The microstructure in Fig. 3(a) corresponds to the unsensitized region and 3(b) to the sensitized region.

The microstructural changes with heat treatment at 600 °C (873 K) are shown in Figs. 4(a)–(c), for treatment times of 1 h, 2 h and 3 h respectively. Here Fig. 4(a) shows delta ferrite lined with carbide

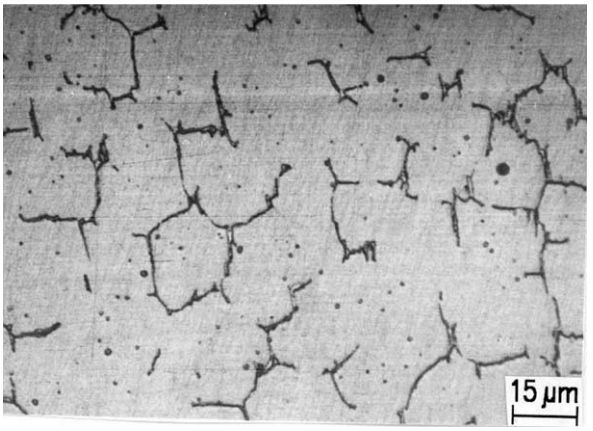

Fig. 2. Optical micrograph showing the initial microstructure of modified 316N SS weld metal (delta ferrite with vermicular morphology).

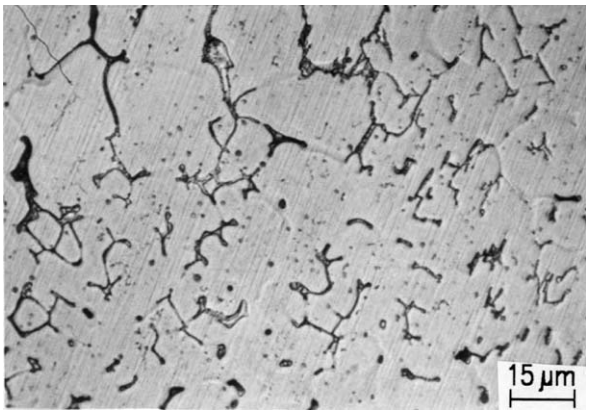

Fig. 3(a). Optical micrograph of modified 316N SS weld metal aged at 525 °C (798 K) for 10 h showing delta ferrite and carbides at delta/austenite boundaries.

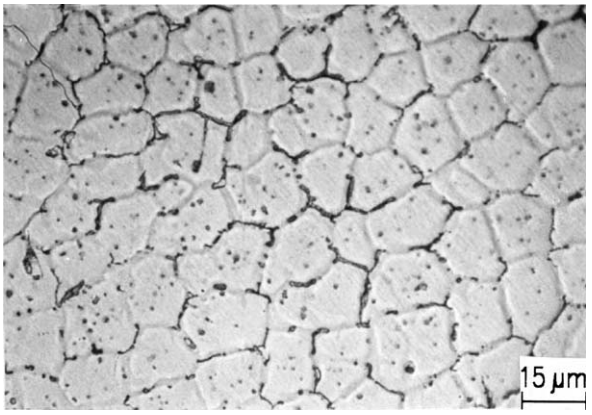

Fig. 3(b). Optical micrograph of modified 316N SS weld metal aged at 525 °C (798 K) for 15 h showing carbides at intercellular regions.

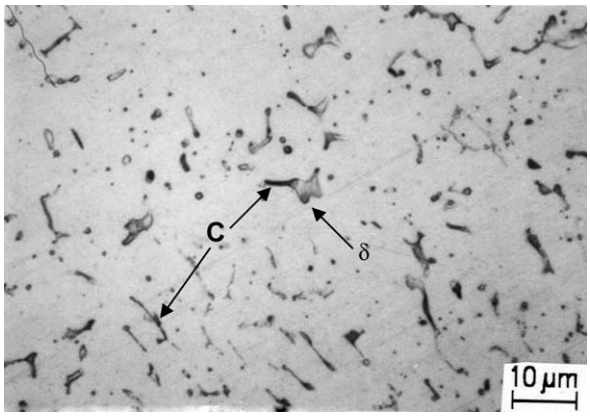

Fig. 4(a). Optical micrograph of modified 316N SS weld metal aged at 600 °C (873 K) for 1 h showing carbides (dark regions marked C) and untransformed delta ferrite.

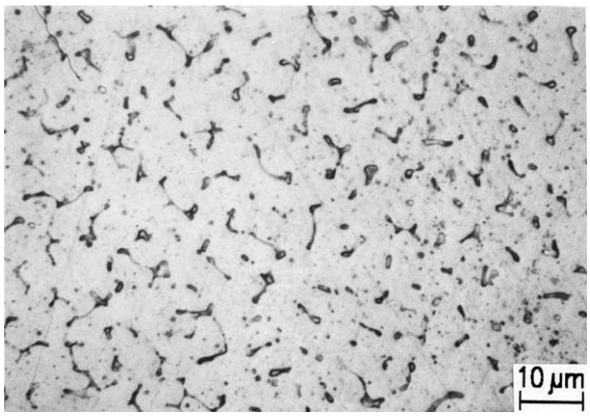

Fig. 4(b). Optical micrograph of modified 316N SS weld metal aged at 600 °C (873 K) for 2 h showing discrete carbides and break up of delta ferrite.

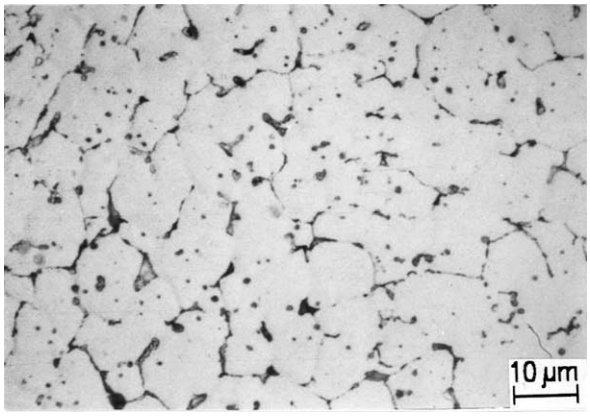

Fig. 4(c). Optical micrograph of modified 316N SS weld metal aged at 600 °C (873 K) for 3 h showing coarsening of carbides.

film in some areas (dark boundaries) and the delta ferrite shows considerable signs of transformation. After 2 h (Fig. 4(b)) the breakup of delta ferrite is more advanced and carbide films have broken up into discrete particles that have coarsened and are present throughout the microstructure. When ageing is further continued for 3 h, the carbide particles have coarsened appreciably. The series of three micrographs corresponds to the progression from unsensitized, to nearly sensitized to sensitized microstructure. The association of delta ferrite with absence of sensitization and its disappearance with sensitization is therefore clear. X-ray diffraction analysis of extracted precipitates of a specimen aged at 600 °C (873 K) for 10 h confirmed that $M_{23}C_6$ carbide was the most predominant phase present and delta ferrite was absent in the sensitized condition.

An extreme case where delta ferrite was totally absent in the sensitized microstructure is shown in Fig. 5, which shows a specimen aged at 650 °C (923 K) for 10 h. Here, the austenite grain boundaries have been decorated extensively with coarse carbide precipitates. (The round particles in the microstructure are slag inclusions from the welding flux, as confirmed by EDAX analysis.) This type of grain boundary precipitation is typically found in single-phase austenitic base metal and is associated with sensitization.

At higher temperatures of ageing such as 850 °C (1123 K), delta ferrite almost completely transforms to sigma phase, as illustrated in Fig. 6. Any carbide precipitation that is observed is likely to have already formed during multipass welding, as it does

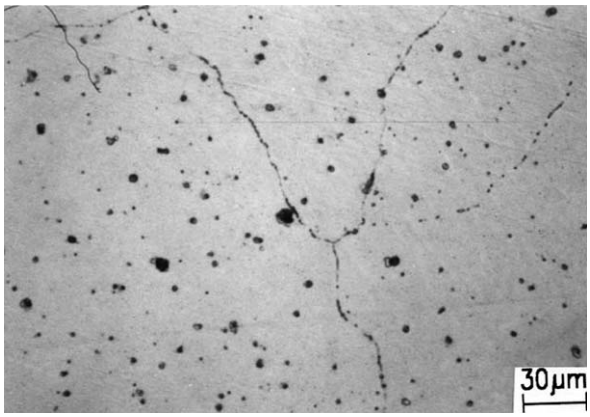

Fig. 5. Optical micrograph of modified 316N SS weld metal aged at 650 °C (923 K) for 10 h showing austenite grain boundaries being decorated with coarse carbides.

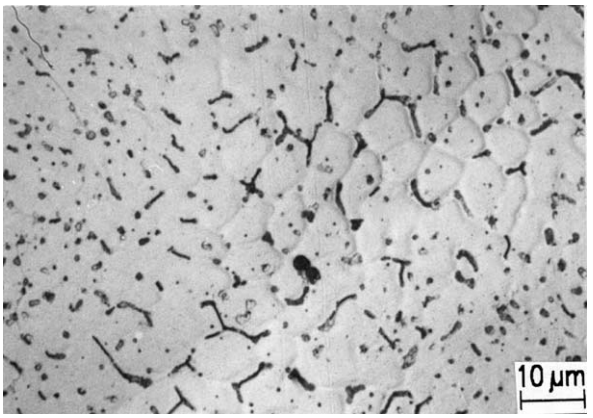

Fig. 6. Optical micrograph of modified 316N SS weld metal aged at 850 °C (1123 K) for 1 h showing sigma phase.

not redissolve at this temperature. The extracted precipitate for a specimen aged at 850 °C (1123 K) for 1 h showed predominantly sigma phase, although some $M_{23}C_6$ as remnant of the unaged multipass weld microstructure is possible.

The fractograph of the specimen aged at 600 °C (873 K) for 10 h and subjected to ASTM A262 Practice *E* test is presented in Fig. 7. As illustrated in this figure, fracture along interdendritic regions has been observed in sensitized weld metal all along the edges. At the centre of the specimen ductile fracture was observed. This is in contrast to the intergranular fracture along the austenite grain boundaries usually observed in the HAZ of austenitic stainless steel base metals. The association of the chromium depletion with the dendritic structure is because of the carbide precipitation at these boundaries, where delta ferrite was also present.

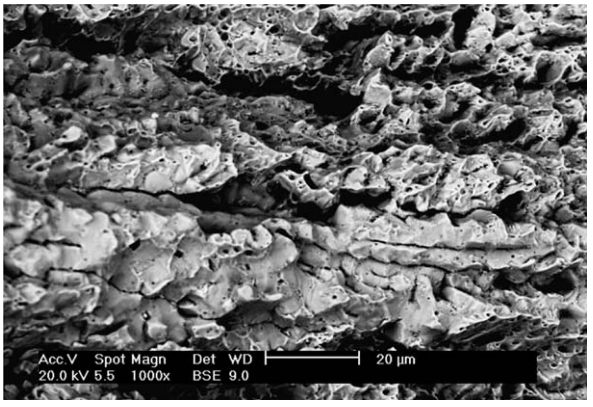

Fig. 7. Fractograph of modified 316N SS weld specimen aged at 600 °C (873 K) for 100 h and subjected to ASTM A262 Practice *E* test showing fracture along interdendritic features.

3.2.2. Modified 316L SS weld metal

The initial microstructure of modified 316L SS weld metal is presented in Fig. 8. The as-deposited weld metal showed a discontinuous network of delta ferrite of vermicular morphology. The delta ferrite was estimated to be in the range of 8–11 FN. When heat treated at 625 °C (898 K) for 50 h, delta ferrite content decreased to 5.27 FN and Fig. 9(a) shows microstructure obtained after etching in oxalic acid indicating delta ferrite lined with carbide film. Fig. 10(a) is the corresponding microstructure after etching in modified Murakami reagent which shows sigma phase precipitated within delta ferrite through out the specimen. In this etchant, matrix and ferrite phases are stained light and medium tan colour respectively and sigma is stained reddish brown colour. Transformation of delta ferrite and appearance of $M_{23}C_6$ and sigma can be clearly seen in Fig. 10(a). Since the carbide network and the associated chromium depletion are discontinuous, the specimen did not fail in ASTM A262 Practice *E* test. Further ageing at the same temperature for 100 h reduces delta ferrite content to 2.7 FN (Table 3). Delta ferrite grains are still present and nearly continuous network of carbides are seen in Fig. 9(b). The corresponding microstructure of the specimens in Fig. 10(b) showing elongated sigma phase. This specimen also did not fail in ASTM A262 Practice *E* test for the same reason explained for the 50 h aged specimen. Extended ageing resulted in IGC attack. Fig. 9(c) shows continuous carbide network and Fig. 10(c) shows more of elongated sigma particles as network. The failure in U

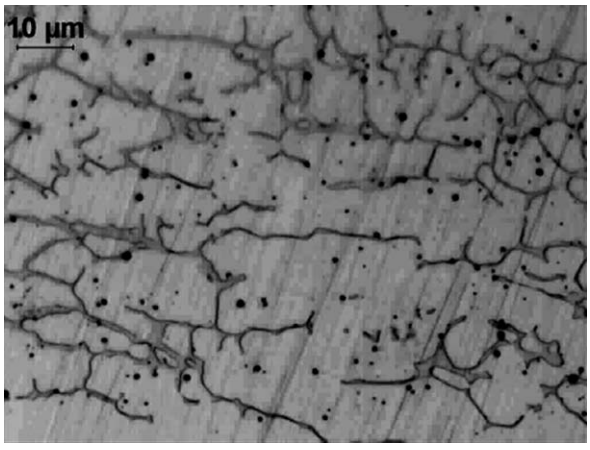

Fig. 8. Optical micrograph showing the initial microstructure of modified 316L SS weld metal (delta ferrite with vermicular morphology).

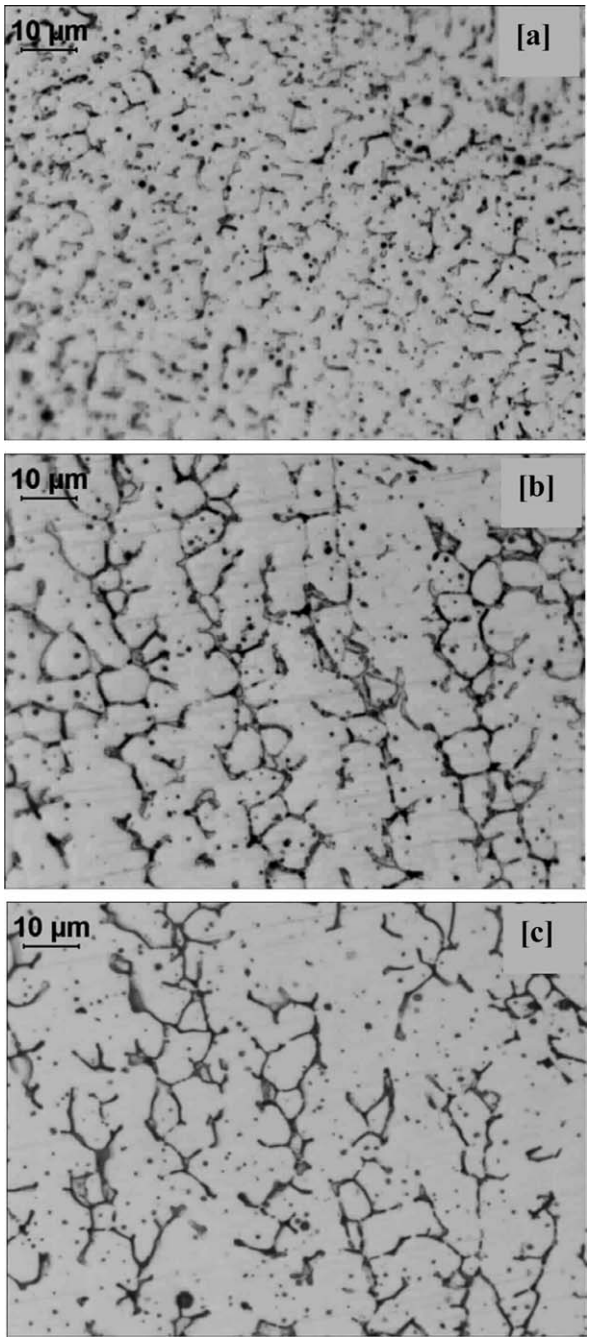

Fig. 9. Microstructure obtained for modified 316L SS weld metal (a) 625 °C (898 K) – 50 h; (b) 625 °C (898 K) – 100 h; (c) 625 °C (898 K) – 200 h (Etchant – 10% oxalic acid).

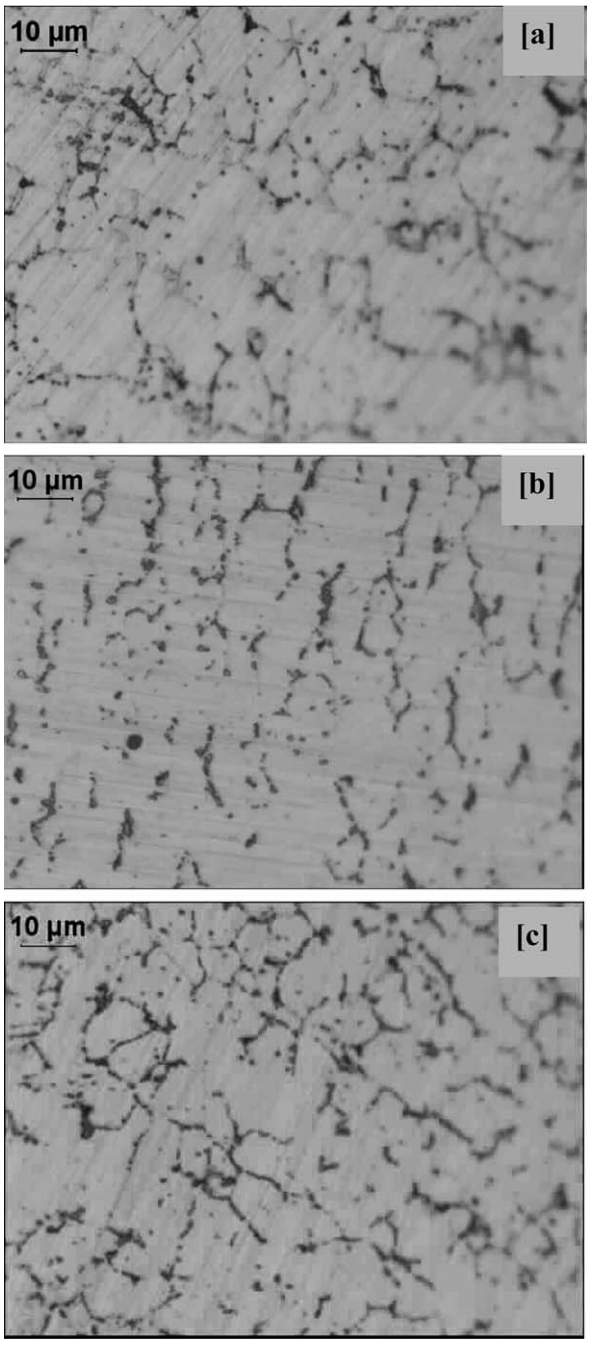

Fig. 10. Microstructure obtained for modified 316L SS weld metal (a) 625 °C (898 K) – 50 h; (b) 625 °C (898 K) – 100 h; (c) 625 °C (898 K) – 200 h; (Etchant – modified Murakami solution).

bend test can be attributed to sensitization and IGC due to Cr depletion and inherent loss in ductility due to sigma formation.

When aged at 650 °C (923 K) for various durations viz., 24 h, 40 h, 50 h and 100 h delta ferrite progressively transforms to carbide and sigma phase as is evident from the FN (Table 3) and the microstructures given in Fig. 11(a–d). Here 40 h itself leads to IGC. When aged at 675 °C (948 K) for 50 h, 100 h and 200 h , the delta ferrite content

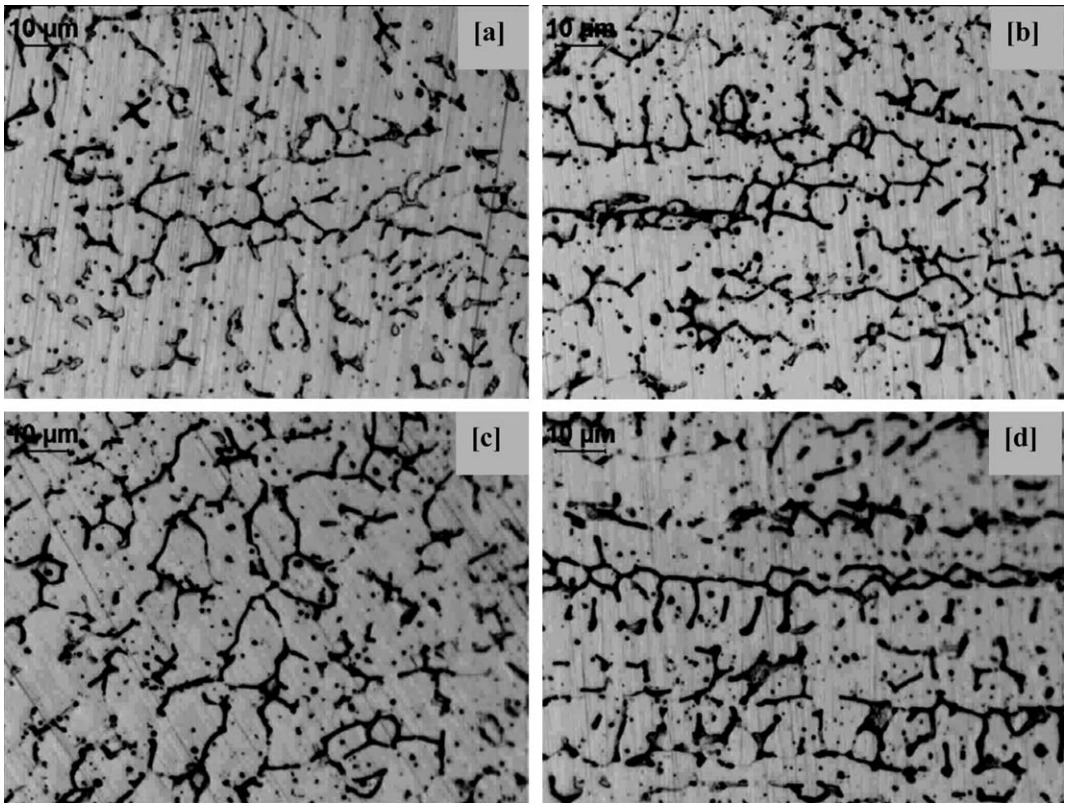

Fig. 11. Microstructure obtained for modified 316L SS weld metal (a) 650 °C (923 K) – 24 h; (b) 650 °C (923 K) – 40 h; (c) 650 °C (923 K) – 50 h (d) 650 °C (923 K) – 100 h; (Etchant – 10% oxalic acid).

changes from 8–11FN to 1.11, 0.36 and 0.04. The microstructures obtained are given in Fig. 12(a)–(c). Of all the 316L SS weld specimens studied, the specimen heat treated at 675 °C (948 K) for 200 h showed the maximum reduction in ductility. After exposure to Strauss test solution, the specimen failed even before doing the bend test. Fig. 13 shows the fracture surface and presence of bulky particles are seen in the fractograph which are identified as sigma by EDAX. Similar to modified 316N SS weld metal, fracture along interdentritic regions has been observed. Intergranular failure along austenite grain boundary was not observed.

From all the above microstructures it can be summarized that thermal ageing of modified 316L SS weld metal results in dissolution of delta ferrite and precipitation of $M_{23}C_6$ along delta ferrite/austenite interfaces as well as sigma phase precipitation within delta ferrite. Carbides are formed initially while isolated sigma particles could be observed towards the end of transformation. Carbon promotes the removal of chromium in the form of $M_{23}C_6$ which proceeds till the carbon potential of the surrounding austenite decreases sufficiently. After that if sufficient chromium is available sigma forms. The amount of sigma phase increases with increase in ageing temperature due to increased diffusivity of sigma forming elements. Initially sigma was present as elongated particles in a discontinuous network. With increase in ageing time and temperature, the network is broken and large spheroidised particles are formed. ASTM A262 Practice *E* test detects susceptibility to IGC associated with $M_{23}C_6$ precipitation and is not intended to detect that due to sigma phase embrittlement. However, in these cases, because of long term high temperature ageing, sigma phase contributes to reduction in ductility even before exposure to the corrodant as per ASTM A262 Practice *E* test. Under such conditions failure in ASTM A262 Practice *E* test has taken place predominantly due to the inherent loss in ductility due to sigma phase embrittlement, while IGC due to chromium depletion played a minor role.

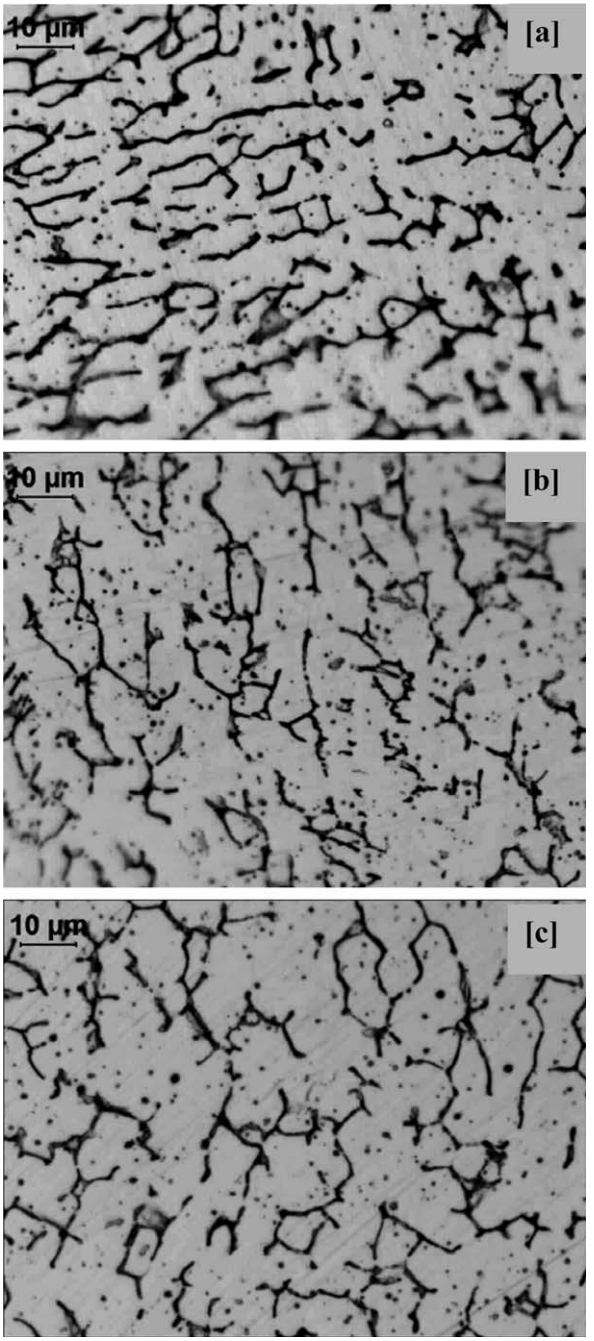

Fig. 12. Microstructure obtained for modified 316L SS weld metal (a) 675 °C (948 K) – 50 h; (b) 675 °C (948 K) – 100 h; (c) 675 °C (948 K) – 200 h; (Etchant – 10% oxalic acid).

3.3. Microstructural evolution and sensitization behaviour

Based on the above microstructural studies, the following differences can be inferred in the sensitization behaviour of single phase austenitic stainless steel and duplex austenite–ferrite stainless steel weld metals. In the case of single phase austenitic stainless steel certain time–temperature combinations will be sufficient to precipitate chromium-rich $M_{23}C_6$ carbide but insufficient to rediffuse chromium back to the depleted zone in the austenite near carbides. This will result in the formation of envelopes of chromium-depleted zones around $M_{23}C_6$ carbides. Since the carbides precipitate along austenite boundaries, the linking of the chromium-depleted zones provides a continuous path of lower corrosion resistance along the grain boundaries for the propagation of IGC.

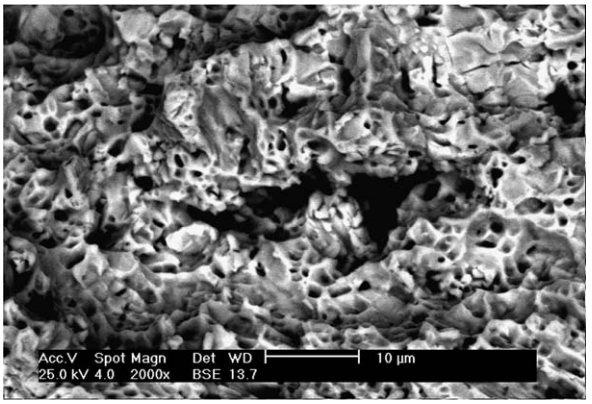

Fig. 13. Fractograph of modified 316L SS weld specimen aged at 675 °C (948 K) for 200 h and subjected to ASTM A262 Practice *E* test showing fracture along interdendritic features.

In the case of duplex weld metal containing austenite and delta ferrite also, thermal exposure in the sensitization range results in $M_{23}C_6$ carbide precipitation. Since chromium diffusion is much faster in ferrite than in austenite, the carbides grow faster in ferrite than in austenite. Consequently, a wide but shallow chromium depleted zone develops on the ferrite side and a very deep but narrow chromium depleted zone develops on the austenite side. Delta ferrite starts transforming to secondary austenite. As long as the delta ferrite present is in contact with the growing carbide, quicker homogenisation of chromium depletion takes place and hence the material will be free from sensitization. However, when delta ferrite transforms more or less completely to $M_{23}C_6$ and secondary austenite, the carbide starts drawing chromium from the surrounding austenitic matrix. This leads to formation of narrow and steep chromium concentration gradients along the austenite grain boundaries and the

material gets sensitized. When the sensitized material is exposed to corrosive medium corrosion takes place along the interdentritic boundaries leading to failure. This mechanism is clearly illustrated by the microstructures shown in Figs. 2–6 and fractograph shown in Fig. 7 and is valid in the temperature range in which carbide precipitation is the predominant mechanism of transformation of delta ferrite. Time to sensitization in the peak temperature range in the present case is influenced greatly by the nitrogen content of the weld metal and the times reported here are much longer than for 316 (base or weld metal compositions) containing less nitrogen. These findings are consistent with the observations of Nakao et al. [13] for AISI type 308 stainless steel, although the kinetics of transformation are much faster in their case because of very low nitrogen levels (<0.01%).

It is interesting that in some cases, the microstructures corresponding to sensitized specimens aged at 650 °C (923 K) showed austenite grain boundaries decorated with carbides. These grain boundaries are not normally visible in duplex stainless steel weld metal because of the strong attack by the etchant on the interphase boundaries in preference to these austenite grain boundaries. In the total absence of delta ferrite, the material essentially behaves as high carbon base material and chromium carbide precipitation at the grain boundaries has therefore resulted in sensitization.

For temperatures of 725 °C (998 K) and above, transformation is predominantly to sigma phase. Sigma phase formation takes place by consumption of chromium present in delta ferrite, with very little or no contribution of chromium from the surrounding austenitic matrix. That is why sigma phase formation alone does not result in sensitization of the microstructure.

4. Validation of CCR of modified 316N and 316L SS weld metals by controlled heating–soaking–cooling trials

4.1. Solution-annealing of modified 316N SS weld metals

For modified 316N SS weld metal subjected to solution-annealing heat treatment (Table 4 – No. 1, 2, 3), heating and cooling up to 65 °C/h results in sensitization whereas 75 °C/h does not lead to sensitization. From the above results, it can be seen that CCR lies between 65 °C/h and 75 °C/h when welded components are cooled from 1050 °C (1323 K). The heating rate is not a concern because the carbides formed during heating part of the heat treatment will be solutionised at 1050 °C (1323 K). Cooling at the rate of 75 °C/h can be safely followed without the risk of sensitization. It is well known that solution-annealing at 1050 °C (1323 K) results in complete dissolution of delta ferrite present in the weld metal and subsequent transformation to austenite. In other words, after solution-annealing the weld metal behaves as base metal (austenitic stainless steel) of higher carbon content. In our earlier investigation, sensitization behaviour of austenitic stainless steel Type 316 having different carbon and nitrogen contents were compared [19]. It was found that for stainless steel containing C-0.054% and N-0.053% [alloy 1] the CCR was determined as 365 °C/h, for C-0.043% and N-0.075% [alloy 2] the CCR was 17 °C/h, and for C-0.03% and N-0.086% the CCR was as low as 0.43 °C/h. These data clearly indicates that lowering the carbon content and increasing the nitrogen content results in significant reduction in the kinetics of sensitization. Since the composition of the weld metal prepared using welding electrode containing 0.045–0.055%C and 0.06–0.1%N is expected to lie in between that of alloy 1 and 2, the CCR for solution annealed weld metal is also expected to lie between 365 °C/h and 17 °C/h and our results are in agreement with this prediction.

Table 4
Details of the controlled heating–soaking–cooling cycles carried out for solution-annealing of modified 316N SS weld metal and results obtained in ASTM A262 Practice *E* test

No.	Heating-holding-cooling cycles	Result obtained in ASTM Practice *E* test
1	Room temperature to 1050 °C (1323 K) in 2 h Hold at 1050 °C (1323 K) for 1 h 1050 °C (1323 K) to Room temperature @50 °C/h	Attack
2	Room temperature to 1050 °C (1323 K) in 2 h Hold at 1050 °C (1323 K) for 1 h 1050 °C (1323 K) to Room temperature @65 °C/h	Attack
3	Room temperature to 1050 °C (1323 K) in 2 h Hold at 1050 °C (1323 K) for 1 h 1050 °C (1323 K) to Room temperature @75 °C/h	No attack

Table 5
Details of the controlled heating–soaking–cooling cycles carried out for stress-relieving of modified 316N SS weld metal and results obtained in ASTM A262 Practice *E* test

No.	Heat treatment	Heating-holding-cooling cycles	Result obtained in ASTM Practice *E* test
1	Stress-relieving	Room temperature to 850 °C (1123 K) @90 °C/h Hold at 850 °C (1123 K) for 4 h 850 °C (1123 K) to Room temperature @90 °C/h	No attack
2	Solution-annealing	Room temperature to 1050 °C (1323 K) in 2 h Hold at 1050 °C (1323 K) for 1 h 1050 °C (1323 K) to Room temperature @90 °C/h, @110 °C/h, @140 °C/h and @200 °C/h	Attack
	Stress-relieving	Room temperature to 850 °C (1123 K) @90 °C/h, @110 °C/h, @140 °C/h and @200 °C/h Hold at 850 °C (1123 K) for 4 h 850 °C (1123 K) to Room temperature @90 °C/h, @110 °C/h, @140 °C/h and @200 °C/h	
3	Solution-annealing	Room temperature to 1050 °C (1323 K) in 2 h Hold at 1050 °C (1323 K) for 1 h 1050 °C (1323 K) to Room temperature @90 °C/h	Attack
	Stress-relieving	Room temperature to 850 °C (1123 K) @90 °C/h Hold at 850 °C (1123 K) for 2 h 850 °C (1123 K) to Room temperature @90 °C/h	
4	Solution-annealing	Room temperature to 1050 °C (1323 K) in 2 h Hold at 1050 °C (1323 K) for 1 h 1050 °C (1323 K) to Room temperature @90 °C/h	Attack
	Stress-relieving	Room temperature to 750 °C(1023 K) @90 °C/h Hold at 750 °C(1023 K) for 4 h 750 °C(1023 K) to Room temperature @90 °C/h	

Table 6
Details of controlled heating–soaking–cooling cycles carried out for modified 316L SS weld metal and results obtained in ASTM A262 Practice *E* test

No.	Heat treatment	Heating–soaking–cooling cycles	Result obtained in ASTM A262 Practice *E* test
1	Solution-annealing [Step 1]	Room temperature to 1050 °C (1323 K) in 2 h Hold at 1050 °C (1323 K) for 1 h 1050 °C (1323 K) to Room temperature @120 °C/h, @50 °C/h, @30 °C/h, @20 °C/h and @10 °C/h	No attack
2	Pre-heating [Step 2]	Room temperature to 500 °C (773 K) @120 °C/h, @50 °C/h, @30 °C/h, @20 °C/h and @10 °C/h Hold at 500 °C (773 K) for 1 h	
3	Stress-relieving [Step 3]	500 °C (773 K) to 850 °C (1123 K) @120 °C/h, @50 °C/h, @30 °C/h, @20 °C/h and @10 °C/h Hold at 850 °C (1123 K) for 4 h 850 °C (1123 K) to Room temperature @120 °C/h, @50 °C/h, @30 °C/h, @20 °C/h and @10 °C/h	
4	Pre-heating after repair [Step 4]	Room temperature to 500 °C (773 K) @120 °C/h, @50 °C/h, @30 °C/h, @20 °C/h and @10 °C/h Hold at 500 °C (773 K) for 1 h	
5	Stress-relieving after repair [Step 5]	500 °C (773 K) to 850 °C (1123 K) @120 °C/h, @50 °C/h, @30 °C/h, @20 °C/h and @10 °C/h Hold at 850 °C (1123 K) for 4 h 850 °C (1123 K) to Room temperature @120 °C/h, @50 °C/h, @30 °C/h, @ 20 °C/h and @10 °C/h	

4.2. Stress-relieving

4.2.1. Single step stress-relieving for modified 316N SS weld metals

For weld metal subjected to stress-relieving heat treatment (Table 5 – No. 1) heating and cooling at the rate of 90 °C/h does not result in sensitization, since this cooling rate is higher than the CCR (75 °C/h).

4.2.2. Two step heat treatment for hard-faced components containing modified 316N SS welds

For the hard-faced components containing modified 316N SS welds which may be subjected to two step heat treatment involving solution-annealing and stress-relieving (Table 5 – No. 2), heating and cooling at various rates of viz., 90 °C/h, 110 °C/h, 140 °C/h and 200 °C/h also resulted in severe sensitization. This is expected because CCR for this

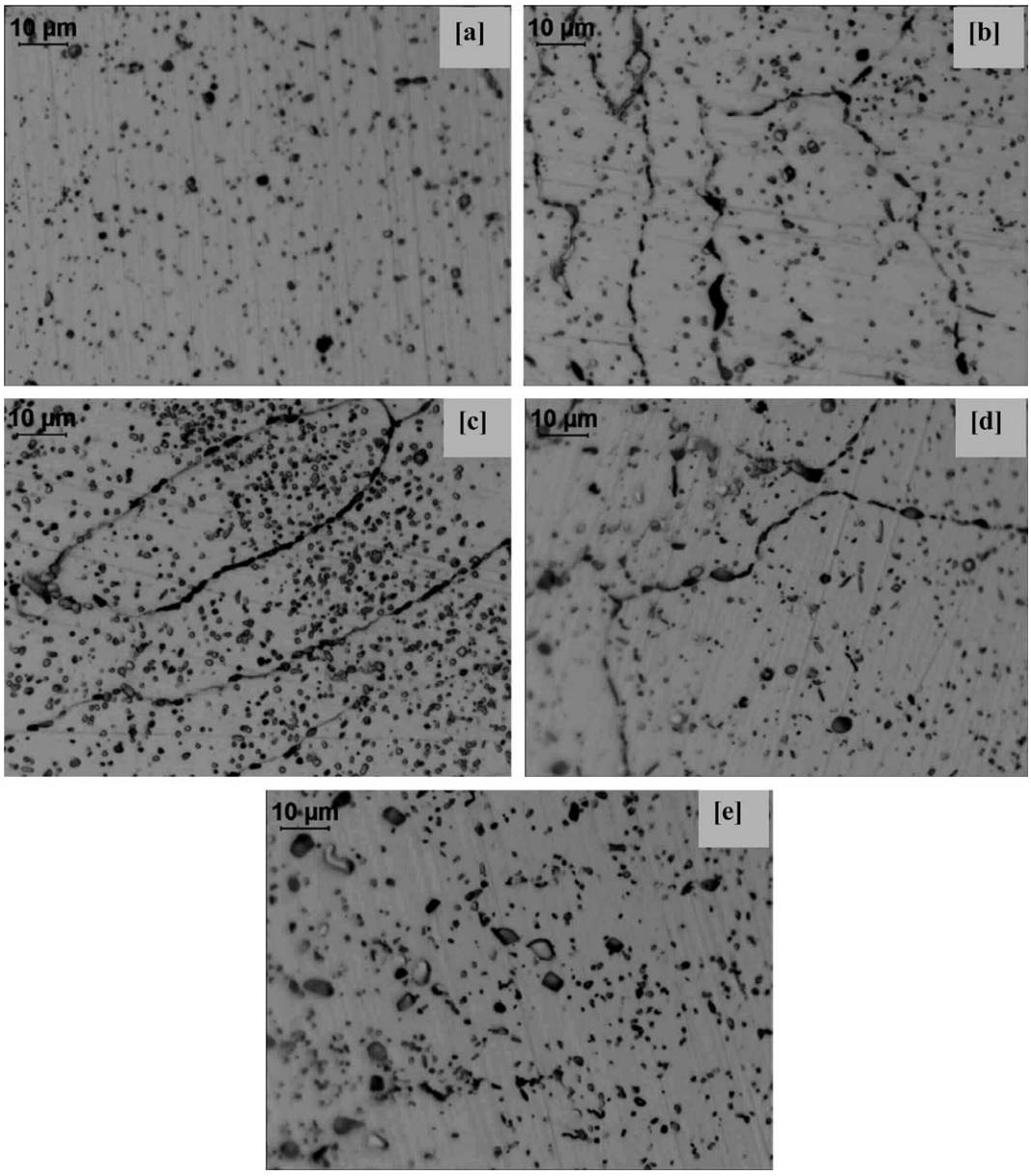

Fig. 14. Microstructure obtained for modified 316L SS weld metal after solution-annealing, stress-relieving and cooling at the rate of (a) 120 °C/h; (b) 50 °C/h; (c) 30 °C/h; (d) 20 °C/h; (e) 10 °C/h (Etchant – 10% oxalic acid).

composition is 75 °C/h (for single phase austenite). As explained in Section 4.1, the heating rate to reach solution-annealing temperature is not a concern because soaking dissolves all the carbides which are nucleated due to the thermal exposure in the sensitization range. However, during cooling, $M_{23}C_6$ nucleates and grows when passing through the sensitization range.

Subsequent stress-relieving exposes the material twice to the sensitization range (heating and cooling). Therefore totally three times the welded component is exposed to the sensitization range and hence three times faster cooling (225 °C/h) only will avoid sensitization.

Since the maximum permissible heating/cooling rate which will retain the desired mechanical property of the hard face coating is 90 °C/h, some more attempts were made to modify the heat treatments either by soaking at 850 °C (1123 K) for a lesser duration viz., 2 h (Table 5 – No. 3) or lower soaking temperature, viz., 750 °C (1023 K) for a longer duration (Table 5 – No. 4) and cooling at 90 °C/h were attempted but all the heat treatment resulted in severe sensitization.

4.3. Stress-relieving of hard faced components containing modified 316L SS welds

From Section 4.2.2 it can be concluded that for hard faced 316LN SS components containing 316L SS welds, indigenously developed modified 316N SS welding electrodes cannot be used because the CCR is very much higher and will certainly lead to reintroduction of residual stress and cracking of hard face deposit. Hence 316L electrodes with lower carbon only will enable stress-relieving heat treatment to be performed at a permissible rate so that sensitization as well as reintroduction of residual stress can be avoided simultaneously. As explained in Section 3.1, CCR for 316L SS weld metal will be about 1 °C/h. This prediction is validated by performing the actual stress-relieving heat treatment envisaged for bottom plate of the grid plate assembly for PFBR as follows:

(1) Solution-annealing at 1050 °C (1323 K).
(2) Pre-heating before hard facing.
(3) Stress-relieving after hard facing.
(4) Pre-heating before repair (assuming that repair is required).
(5) Stress-relieving after repairing the hard face deposit.

The above five steps were simulated as indicated in Table 6 with five different heating and cooling rates, viz., 120 °C/h, 50 °C/h, 30 °C/h, 20 °C/h and 10 °C/h. It has been found that the weld metal does not get sensitized even at the rate of 10 °C/h. The microstructure obtained after the above heat treatment is presented in Fig. 14(a–e) The fastest cooling rate also viz., (120 °C/h) has resulted in isolated carbide precipitation (Fig. 14(a)) and isolated sigma phase. With progressive decrease in heating and cooling rates, the duration of exposure to sensitization regime increases nucleation of carbides along grain boundaries and sigma phase throughout the specimen. Since continuous carbide network and associated chromium depleted zones are not seen in the microstructure it can be concluded that there is no risk of sensitization during the stress relieving treatment for the rates presented in Table 6.

5. Conclusions

The sensitization behaviour of modified 316N SS and 316L SS weld metal prepared using indigenously developed, modified 316N SS electrodes and 316L SS electrodes respectively was established by performing both isothermal and continuous heating and cooling heat treatment cycles. Susceptibility to IGC was assessed by ASTM A262 Practice *E* test. Microstructural changes taking place during various thermal exposures were characterized using optical and scanning electron microscopy studies and electrochemical phase separation and X-ray diffraction techniques. The mechanism of sensitization was explained based on these studies:

1. TTS diagrams were developed for modified 316N SS weld metal and 316L SS weld metal. Modified 316N SS weld metal exhibited sensitization in the temperature 525–725 °C (798–998 K). The minimum time required for sensitization was 25 minutes. The critical cooling rate above which there is no risk of sensitization is 160 °C/h (when cooling starts from 725 °C (998 K)). The 316L SS weld metal gets sensitized in the temperature range of 625 °C (898 K) to 675 °C (948 K). The minimum time required for sensitization at the nose temperature (t_{min}) is about 40 h. From this diagram, CCR above which there is no risk of sensitization, was calculated as 1 °C/h. This value is applicable only when cooling of the weld metal starts from 675 °C (948 K).

2. In both the materials, delta ferrite transforms to $M_{23}C_6$ carbides and austenite. In low carbon weld metal, in addition to carbides, sigma phase is also observed. In modified 316N SS weld metal failure in ASTM A 262 Practice *E* is due to corrosion of chromium depleted zone formed by carbide precipitation whereas in 316L SS weld metal, the loss in ductility due to sigma phase also contributes to the failure in U bend test.
3. For short ageing times prior to onset of sensitization in the critical temperature range, untransformed delta ferrite was present along with $M_{23}C_6$ carbides. In the presence of delta ferrite in close contact, chromium supply for carbide precipitation comes from this phase, which protects the surrounding austenite from chromium depletion.
4. Intergranular attack was not observed in specimens aged above the critical temperature range (for carbide precipitation), in which transformation was predominantly to sigma phase.
5. For modified 316N SS weld metal, when cooling starts from 1050 °C (1323 K) (solution-annealing temperature), the critical cooling rate is 75 °C/h. The difference in the CCR has been attributed to the transformation characteristics of delta ferrite.
6. For the stress-relieving heat treatment of hard faced components containing weld metal fabricated with modified 316N indigenous electrode, heating/cooling at the rate of 200 °C/h also results in sensitization. Since solution-annealing followed by stress-relieving at a heating/cooling rate above CCR will certainly lead to reintroduction of the residual stress and cracking of hard face deposit, welding electrode of such high carbon should not be used wherever hard facing and double heat treatment are required. Use of electrodes of lower carbon is expected to solve the problem.

Acknowledgements

The authors are grateful to Dr Baldev Raj, Director, Indira Gandhi Centre for Atomic Research, Dr S.L. Mannan, Director, Metallurgy and Materials Group, Dr V.S. Raghunathan, Associate Director, Materials Characterisation Group, for their keen interest and support during the course of the investigation. The authors gratefully acknowledge the assistance provided by Mr M. Sangiah in carrying out heat treatments and Mrs K. Parimala in carrying out corrosion tests. The authors thank Mr K.Thyagarajan for his help in preparing the line drawing.

References

[1] S.K. Ray, V. Shankar, V. Balasubramaniam, V.K. Sethi, Heat treatment of Austenitic Stainless steel components, in: Proceedings of the Seminar Materials R&D for PFBR held on 1–2 January 2003, p. 215.
[2] ASM committee on Heat Treating, Metals Hand Book, 9th Ed., ASM, Metals Park, OH, 1981, p. 647.
[3] V. Cihal, Intergranular Corrosion of steel and alloysMaterial Science Monograph, vol. 18, Elsevier, New York, NY, 1984.
[4] A.J. Sedricks, Corrosion of Stainless Steel, 2nd Ed., John Wiley, NY, 1996.
[5] E. Folkhard, Welding Metallurgy of Stainless Steel, Springer-Verlag, Vienna, 1988.
[6] H.E. Hannien, Int. Met. Rev 3 (1979) 85.
[7] E.A. Trillo, L.E. Murr, Acta Mater. 47 (1) (1999) 235.
[8] H.D. Solomon, T.M. Devine Jr., in: Proceedings of the Conference on Duplex Stainless Steels, American Society for Metals, Metals Park, OH, 1983, p. 693.
[9] E. Angelini, B. Benedetti, G. Maizza, F. Rossalbino, Corrosion 55 (6) (1999) 606.
[10] E. Erauzkin, A.M. Irisarri, in: Applications of Stainless Steels '92, vol. 2, Stockholm, Sweden, 9–11 June 1992, p. 870.
[11] H. Menendez, T.M. Devine, Corrosion 46 (5) (1990) 410.
[12] C.D. Lundin, Maintenance and Repair Welding in Power Plants, Orlando, FL, USA, 9–11 December 1991, p. 46.
[13] Y. Nakao, K. Nishimoto, M. Ishizaki, Welding Int. 6 (7) (1992) 523.
[14] T.P.S. Gill, R.K. Dayal, J.B. Gnanamoorthy, Welding J. 9 (1979) 3755.
[15] Recommended Practices for Detecting Susceptibility to Intergranular corrosion in Stainless Steels, A-262-02; ASTM Annual Book, vol. 3.02, ASTM Publications, Philadelphia, 2003.
[16] R.K. Dayal, J.B. Gnanamoorthy, Corrosion 36 (1980) 104.
[17] T.P.S. Gill, M. Vijayalakshmi, V. Shankar, P. Rodriguez, Scr. Metall. Mater. 27 (1992) 313.
[18] T.P.S. Gill, V. Shankar, M.G. Pujar, P. Rodriguez, Scr. Metall. Mater. 32 (1995) 1595.
[19] N. Parvathavarthini, R.K. Dayal, J. Nucl. Mater. 305 (2002) 209.